

Elastic Scattering of Slow Electrons by Two-Electron Ions

M. R. C. McDowell*†

Goddard Space Flight Center, Greenbelt, Maryland

(Received 8 April 1968; revised manuscript received 2 July 1968)

A one-channel model, previously used for He, is extended to allow calculation of elastic scattering by H^- and Li^+ at energies up to 3 Ry. Nonseparable ground-state wave functions are used, allowance being made for exchange, and dipole and quadrupole polarization potentials. Results for Li^+ are in good agreement with quantum-defect-method values. Calculated differential cross sections for elastic scattering by H^- at energies of $\frac{1}{2}$ and 1 Ry are presented. Deviations from Coulomb scattering are marked. Phase shifts ($l=0, 1$) for higher members of the isoelectronic sequence ($4 \leq Z \leq 10$) are given at threshold and 1 Ry.

I. INTRODUCTION

A considerable number of theoretical investigations on elastic scattering of slow electrons by He atoms¹⁻⁴ have been reported recently. They are in substantial agreement with each other, and are consistent (in the sense of dispersion relations³) with experimental data,^{5,6} except at small scattering angles at energies of 10 eV and below. In view of advances in experimental technique which have allowed measurement^{7,8} of inelastic collision cross sections of slow electrons with H^- (in good agreement with theory⁹), it is of interest to examine elastic scattering by two-electron ions.

In this paper the model of Williamson and McDowell² has been extended and applied to elastic scattering by H^- , Li^+ at energies up to 3 Ry. Some results are also given for higher members of the isoelectronic sequence. The theory is outlined in Sec. II, and the numerical methods employed are discussed in Sec. III. Phase shifts and scattered intensities are presented in Sec. IV, and in the case of Li^+ are compared with the result of a Hartree-Fock calculation,¹⁰ and the quantum-defect method. The work is summarized, and conclusions are presented in Sec. V.

II. THEORY

We consider an electron scattered by a two-electron system of charge Z . The total three-electron system is described by the Schrödinger equation,

$$(H - E)\Psi(1, 2, 3) = 0, \quad (1)$$

with Hamiltonian operator¹¹

$$H = \sum_{i=1}^3 \left(-\frac{1}{2} \nabla_i^2 - \frac{Z}{r_i} \right) + \sum_{i>j} \frac{1}{r_{ij}} \quad (2)$$

In our model the total wave function $\Psi(123)$ is represented by an ansatz,

$$\Psi(1, 2, 3) = \sum_{1,2,3} \psi_0(1, 2) F(3) S(123), \quad (3)$$

where $\psi_0(1, 2)$ is a wave function for the ground state of the target when electrons 1 and 2 are bound, $S(123)$ is a spin function, and $F(3)$ the unknown scattering function to be determined, and

the sum is over cyclic permutations. Taking

$$S(123) = (1/\sqrt{2})(\alpha_1\beta_2 - \alpha_2\beta_1)\alpha_3, \quad (4)$$

where α, β are the one-electron spin-up and spin-down functions, we may write, in a usual notation

$$F(3) = \sum_{l=0}^{\infty} \frac{f_l(3)}{r_3} P_l(\mu_3), \quad (5)$$

the position vector of electron 3 with respect to the target nucleus being

$$\vec{r}_3 = (r_3, \theta_3, \phi_3) \text{ and } \mu_3 = \cos \theta_3.$$

The integrodifferential equation for the scattering functions $f_l(r_3)$ is obtained by projecting out (1) on each partial wave in turn,

$$\int \psi_0^*(1, 2) P_l^*(\mu_3) S^*(123) [H - E] \times \Psi(123) d\vec{r}_1 d\vec{r}_2 d\vec{r}_3 d\text{Spin} = 0. \quad (6)$$

For simplicity we assume that the ground-state function for the target is known exactly

$$\left(-\frac{1}{2} \nabla_1^2 - \frac{1}{2} \nabla_2^2 - \frac{Z}{r_1} - \frac{Z}{r_2} + \frac{1}{r_{12}} \right) \psi_0(12) = E_Z \psi_0(12) \quad (7)$$

$$\text{and } 2E = 2E_Z + k^2. \quad (8)$$

We adopt a two-parameter¹² variational trial function

$$\psi_0(12) = N(e^{-\alpha r_1 - \beta r_2} + e^{-\beta r_1 - \alpha r_2}), \quad (9)$$

for $Z = 1, 2, 3$.

Then, on carrying out the angular and spin integrations, (6) yields

$$L_l^{(0)} f_l(\vec{r}_3) = \frac{16\pi^2 N}{(2l+1)} \left[\delta_{0l} \int_0^\infty \int_0^\infty f_0(1) Z_{00}(123) dr_1 dr_2 - 2 \int_0^\infty \int_0^\infty f_l(1) X_{0l}(123) dr_1 dr_2 \right] = R_l(r_3), \quad (10a)$$

where $L_l^{(0)}$ is the operator

$$L_l^{(0)} = d^2/dr^2 + k^2 - l(l+1)/r^2 - V_{00}(3). \quad (11)$$

The direct and exchange potentials are

$$V_{00}(r) = -\frac{2Z}{r} + \frac{4\pi^2 N^2}{\alpha^3 \beta^3 r} \left([1 - (1 + \alpha r)e^{-\alpha r}] + [1 - (1 + \beta r)e^{-\beta r}] + \frac{128\alpha^3 \beta^3}{(\alpha + \beta)^6} \left\{ 1 - [1 + \frac{1}{2}(\alpha + \beta)r]e^{-(\alpha + \beta)r} \right\} \right),$$

$$Z_{00} = (r_3/N)\psi_0^*(23)r_2^2[(\alpha^2 r_1 - 2\alpha)e^{-\alpha r_1 - \beta r_2} + (\beta^2 r_1 - 2\beta)e^{-\beta r_1 - \alpha r_2} + (1/N) \times \psi_0(12)(r_1 k^2 + 2Z - 2r_1/r_{12}, 0)] \quad (12)$$

$$X_{0l} = r_1 r_3 r_2^2 \psi_0^*(12)(2/r_{13}, l)\psi_0(23),$$

$$r_{13, l} = \left(r < \frac{l}{r} > \frac{l+1}{13} \right)$$

No account has been taken of the polarizability of the target in this model, so we replace $L_l^{(0)}$ by

$$L_l = L_l^{(0)} - 2(v_d + v_q), \quad (13)$$

where v_d and v_q are potentials behaving as r^{-4} and r^{-6} respectively at large r . They are chosen in the Bethe-Reeh form¹³

$$v_d(r) = -(9/2u^4) \left[1 - \frac{1}{3}e^{-2u} (1 + 2u + 6u^2 + \frac{20}{3}u^3 + \frac{4}{3}u^4 - \frac{2}{3}e^{-4u}(1+u)^4) \right],$$

$$v_q(r) = -(15/2y^6) \left[1 - 2y e^{-2y} (1 + 2y + \frac{4}{3}y^2 + \frac{1}{3}y^3 + \frac{2}{9}y^4 + \frac{1}{9}y^5 + \frac{1}{18}y^6 - \frac{1}{175}y^7 + \frac{1}{135}y^8 - \frac{2}{135}y^9) + e^{-4y} (1 + 4y + \frac{20}{9}y^2 + 6y^3 + \frac{28}{9}y^4 + \frac{8}{9}y^5 + \frac{1}{9}y^6) + \frac{8}{135}y^{10} \text{Ei}(-2y) \right], \quad (14)$$

where $\text{Ei}(-u) = -E_1(u)$ and $E_1(u)$ is the exponential integral,¹⁴

$$u = Z_1 r, \quad y = Z_2 r. \quad (15)$$

The parameters Z_1, Z_2 are chosen so $Z_1^4 = 9/\alpha_d$, $Z_2^6 = 15/\alpha_q$, where α_d, α_q are the dipole and quadrupole polarizabilities of the target respectively.

III. NUMERICAL METHODS

The integrodifferential equation

$$L_l f_l(r) = R_l(r) \quad (10b)$$

must be solved subject to the boundary conditions

$$f_l(0) = 0,$$

$$f_l(r) \underset{r \rightarrow \infty}{\sim} k^{-1/2} \sin[kr + (Z_0/k) \ln 2kr - \frac{1}{2}l\pi + \sigma_l + \eta_l] \quad (16)$$

$$\text{with } \sigma_l = \arg \Gamma(l+1 - iZ_0/R)$$

and $Z_0 = (Z-2)$. The quantity of interest is the non-Coulomb part of the phase shift η_l . We shall refer to it simply as the phase shift (for the l th partial wave).

Equation (10b) was solved by a noniterative method. Writing

$$f_l(r) = P(r) + \mu Q(r) + \nu R(r), \quad (17)$$

where P, Q, R , satisfy

$$L_l P = F(P), \quad L_l Q = F(Q) + c_l r^{l+1} e^{-\alpha r}, \quad (18)$$

$$L_l R = F(R) + c_l r^{l+1} e^{-\beta r}, \quad c_l = \frac{16\pi^2 N^2}{(2l+1)}$$

and $F(\phi)$ involves linear combinations of integrals over the range $(0, r)$ only, the parameters μ, ν may be determined in terms of certain infinite integrals once $P(r), Q(r)$, and $R(r)$ are known. For He this procedure yields phase shifts identical to those obtained previously² by an iterative method. The ordinary differential equations (18) were solved by a Fox-Goodwin predictor-corrector method.

The differential equations were integrated out from $r=0$, the first four points being obtained from powers-series solutions, at an interval H_1 . The Fox-Goodwin method is started by computing the solution at the fourth point from the powers-series values at the second and third. If this estimate does not agree with the powers-series value, the initial interval is halved. Otherwise the solution is carried out to the fortieth point, the interval doubled, and a further 100 points computed at interval H_2 , 100 at $H_3 = 2H_2$, and finally 200 at $H_4 = 2H_3 = 8H_1$. For each value of k and l , at least two values of H_1 were used. The asymptotic amplitudes were stable to five significant figures, and the phase shift (modulo π) to three significant figures. Some representative values for the case of H^- (the quadrupole polarizability being set equal to zero) are shown in Table I.

The solutions were normalized by the Strömrgren procedure.¹⁵ The usual method of obtaining the phase shift by matching the solution to a linear combination of regular and irregular Coulomb functions is unsatisfactory close to threshold,¹⁵ particularly when a long-range polarization potential is present. Burgess¹⁵ has given an alternative analytic procedure which is rapidly convergent at all energies. His procedure for determining the phase shift when a polarization potential is present may be extended easily to the case of a negative ion ($Z_0 = -1$).

At large r ,

$$f_l(r) \underset{r \rightarrow \infty}{\sim} k^{-1/2} \sin[\phi(r) + \eta_l] \quad (19)$$

TABLE I. Stability of the computed values of $\tan\eta_l$ for $e\text{-H}^-$ scattering, using the method discussed in the text for different initial intervals H_1 , and selected values of k^2 , l , with $\alpha_q=0$.

$k^2(\text{Ry})$	l	H_1	
		0.05	0.06
0.05	0	8.192, -3	8.191, -3
0.06	0	1.264, -2	1.262, -2
0.10	0	4.056, -2	4.052, -2
		H_1	
		0.025	0.030
0.25	0	2.215, -1	2.215, -1
0.25	1	8.912, -1	8.914, -1
1.0	1	-5.655	-5.646
1.0	2	2.017	2.018
2.25	2	1.858	1.858

where to sufficient accuracy

$$\phi(r) = \phi_1(r) + \frac{1}{2}\Phi(r).$$

Defining

$$\rho = |Z_0 r|, \quad \beta = |Z_0 k|,$$

we have (the \pm sign being that of Z_0),

$$\begin{aligned} \phi_1^\pm = & \chi(\rho)^\pm \pm \beta^{-1} \ln[(\beta^2 \rho + \beta \chi^\pm \pm 1)/\beta] - \frac{1}{2} \rho \pi + \sigma_l^\mp \beta^{-1} \\ & \pm \frac{5(\rho \mp c)}{24\chi(\pm)^3} - \frac{\chi^\pm (3\beta^2 + 4) + \beta\rho(3\beta^2 c + 2) \pm \beta c}{24\chi(1 + \beta^2 c)(\chi^\pm \pm \beta\rho)} \\ & + \left(\frac{c + \frac{1}{8}}{\sqrt{c}}\right) \cos^{-1} T^\pm(\rho), \end{aligned} \quad (20)$$

with

$$\chi^\pm = +(\beta^2 \rho^2 \pm 2\rho - c)^{1/2}, \quad c = l(l+1),$$

$$T^\pm(\rho) = (\beta c \chi^\pm \mp c + \rho)/\rho(1 + \beta^2 c).$$

The polarization term is

$$\begin{aligned} \Phi(\rho) = & \frac{Z_0^2 \alpha_d}{4c^2} \left(\frac{3(2\rho \mp c)}{\rho(\chi^\pm \pm \beta\rho)} + \frac{c\chi^\pm}{\rho^2} \right. \\ & \left. - \frac{(3 + \beta^2 c)}{\sqrt{c}} \cos^{-1} T^\pm(\rho) \right), \quad c \neq 0 \\ = & -\frac{2Z_0^2 \alpha_d (9\beta\rho\chi^\pm + 11\beta^2\rho^2 \pm 6\rho)}{15\rho^2(\chi^\pm \pm \beta\rho)^3}, \quad c = 0. \end{aligned} \quad (21)$$

When $c=0$ the \cos^{-1} term in (20) is replaced by $0.25(\chi^\pm \pm \beta\rho)^{-1}$. No special treatment of the quadrupole potential is required. Dipole and quadrupole polarizabilities for H^- are given by Stewart.¹⁶ The value of the quadrupole polarizability used is uncertain by $\pm 20\%$. The adopted parameters for H^- and Li^+ are displayed in Table II. The dipole polarizability used for Li^+ is the Hartree-Fock value of Lahiri and Mukkerji¹⁷;

TABLE II. Parameters for H^- , Li^+ .

	α	β	α_d	α_q	Z	Z_0
H^-	1.04	0.2808	203	1300	1	-1
Li^+	3.295	2.079	0.19	0	3	+1

its quadrupole polarizability was taken as zero.

IV. RESULTS AND DISCUSSION

The calculated phase shifts for H^- are shown in Tables III-VI. The program actually calculates $\tan\eta_l$, and $\eta_l \pmod{\pi}$. The calculations indicated that if the phase shift was defined to go to zero in the high-energy limit, then the s -wave phase shift must be chosen to be π in the zero-energy limit. This was confirmed by comparing the numerical solution for $k^2=0.05$, $l=0$ with the corresponding pure Coulomb solution. An extra node is present in the calculated solution at small r .¹⁸ Physically this occurs because the incoming electron cannot enter the filled $1s$ shell, and there is, in our model, no bound $(1s)^2 2s$ state of H^- . A similar situation occurs for electron scattering by He, but not for Li^+ . In the latter case the $(1s)^2 2s$ state is the ground-state configuration of Li, and the zero-energy s -wave phase shift is found to be $1.261 \pmod{\pi}$.

We conjecture that the actual zero-energy phase shift is $\pi + 1.261$. This is in accord with a recent extension of Swan's theorem,^{18,19} that for electron scattering by positive ions $\eta_l(\infty) - \eta_l(0) = (m_l + q_l)\pi$, where m_l is the number of bound states of angular momentum l excluded by the Pauli principle, and q_l is, in general, not an integer. The calculated phase shifts for H^- , He, and Li^+ are shown in Fig. 1 (α_q being taken as zero for He and Li^+), that for Li^+ being plotted modulo π for convenience. The agreement of the calculated He phase shifts with those obtained previously by an iterative solution,² and by other authors in similar models^{1,3} is satisfactory. The zero-energy phase shift for Li^+ (modulo π) of 1.261 agrees well with a value, ob-

TABLE III. s -wave phase shifts for H^- .

$k^2(\text{Ry})$	$\tan\eta_0$		η_0
	d^a	$d+q^b$	
0.05	8.19, -3	8.22, -3	3.150
0.06	1.26, -2	1.27, -2	3.154
0.07	1.84, -2	1.85, -2	3.160
0.08	2.51, -2	2.54, -2	3.167
0.09	3.26, -2	3.31, -2	3.175
0.10	4.06, -2	4.13, -2	3.183
0.25	2.22, -1	2.50, -1	3.389
0.50	4.71, -1	5.59, -1	3.650
0.75	3.49, -1	4.20, -1	3.540
1.0	1.74, -1	2.30, -1	3.369
2.0	-3.49, -1	-3.07, -1	2.844
3.0	-7.43, -1	-6.97, -1	2.533

^a d indicates dipole potential only.

^b $d+q$ indicates dipole plus quadrupole potentials.

TABLE IV. Calculated H^- phase shifts (notation as in Table III).

k^2 (Ry)	$l=1$		$l=2$	
	d	$d+q$	d	$d+q$
0.10	4.32, -2	4.38, -2	2.95, -2	2.99, -2
0.15	1.49, -1	1.53, -1	7.41, -2	8.08, -2
0.20	3.72, -1	4.00, -1	1.59, -1	1.63, -1
0.25	7.28, -1	8.12, -1	2.64, -1	2.76, -1
0.50	1.71	1.82	8.13, -1	8.78, -1
0.75	1.78	1.86	1.04	1.11
1.0	1.75	1.82	1.11	1.18
1.5	1.65	1.70	1.12	1.17
2.0	1.57	1.61	1.09	1.14
3.0	1.44	1.46	1.03	1.07

tained using the quantum-defect method²⁰ and tables of atomic energy levels, of $\eta_0(0) = 1.254 \pm 0.005$. The slight discrepancy may be attributed in part to uncertainties in the available values of the dipole polarizability of Li^+ , and the high s -state energies of Li .

Higher terms in the multipole expansion of the adiabatic polarization potential might be expected to be of importance for systems with large static polarizabilities such as H^- . In fact, only the quadrupole component of this potential significantly modifies the usual dipole approximation, and its effects are noticeably only over a small range of r . The local potentials for H^- given by Eqs. (12) and (14) are shown in Fig. 2. The quadrupole component $V_q(r)$ is important within the range $a_0 \leq r \leq 5a_0$ only. The incoming electron sees a repulsive Coulomb potential at large r which is strongly modified by the attractive polarization potentials around $r=10a_0$, becoming attractive at $r=10a_0$, and going over to a Coulomb attraction for $r < a_0$. Exchange effectively increases the attractive part of the potential for $r < 10a_0$.

The local potential shows a broad positive maximum of magnitude ≈ 0.2 Ry, indicating the possibility of trapping of low-energy electrons. The corresponding local potential for electrons incident on He is more attractive, but not sufficiently so to produce an s -wave resonance. However, Herzenberg and Lau²¹ using our model, but with a simpler form of polarization potential, have been able to induce such a resonance by suitably modifying the strength of the exchange term. Peterkop²² has also reported such a resonance at $k = 1.25$ in a one-channel

TABLE V. Calculated H^- phase shifts (dipole-plus-quadrupole potentials only).

k^2 (Ry)	$l=3$	$l=4$	$l=4$ no exchange
0.25	0.139	0.0798	...
0.5	0.400	0.221	0.230
0.75	0.667	0.403	0.390
1.0	0.768	0.503	0.497
1.5	0.858	0.624	...
2.0	0.869	0.669	...
3.0	0.846	0.687	0.687

TABLE VI. Phase shifts for H^- , $l \geq 4$, no exchange (dipole-plus-quadrupole potential only).

k^2 (Ry) \ l	4	5	6	7	8	9	10
0.50	0.230	0.147	0.0944	0.0637	0.0449	0.0327	0.0244
0.75	0.390	0.244	0.158	0.107	0.075	0.0540	0.0403
1.0	0.497	0.329	0.221	0.152	0.107	0.0775	0.0577
3.0	0.687	0.552	0.447	0.360	0.288	0.231	0.185

model of e -He scattering, using a target ground-state wave function containing polarization terms. In view of these results, we made a search for an s -wave resonance in e - H^- scattering in the range $0.05 \leq k^2 \leq 0.2$ Ry at intervals of 0.01 in k^2 (i.e. 0.136 eV). None was found, the values of $\tan \eta_0$ being smoothly varying (cf. Table III) over this range of energies. The search in He was concentrated around $k^2 = 1.5$ Ry, in view of Peterkop's result, but in contrast to Herzenberg and Lau we did not treat the polarizability and the strength of the exchange term as variable parameters. We conclude that no s -wave resonance broader than 0.1 eV exists in our model for either H^- or He. An extension of Peterkop's work on He to H^- using the same type of wavefunction might be worthwhile.

The effect of the quadrupole potential on the s -wave phase shift for H^- is shown in Fig. 3. Selected computed values are also given in Table III. The percentage increases in $\eta_0(k^2) \pmod{\pi}$ on including the quadrupole potential varies from less than 1% ($k^2 < 0.06$ Ry) to 30% at $k^2 = 1.0$ Ry, decreasing to 5% by $k^2 = 3.0$ Ry. The computed phase shifts are stable to better than 1% (cf. Table II). The over-all uncertainty of the tabulated s -wave phase shift, column 4 of Table III, should be less than 10%, and much less than this at small ($k^2 \leq 0.1$ Ry) and high ($k^2 \geq 3.0$ Ry) energies. This uncertainty is due primarily to the uncertainty in the

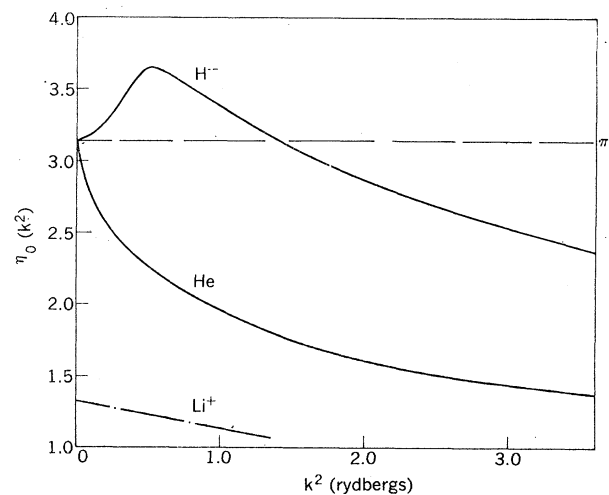


FIG. 1. Calculated s -wave phase shift for elastic scattering of slow electrons by the two-electron systems indicated (dipole polarizability only for He and Li^+ , dipole-plus-quadrupole for H^-).

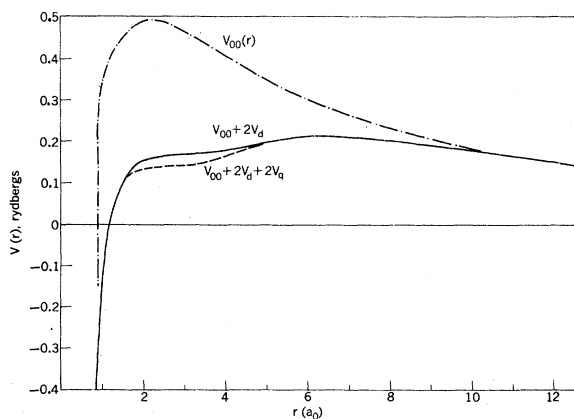


FIG. 2. The local potentials occurring in Eq. (10b) for $Z=1$ (H^-).

available values of α_q , and to neglect of higher multipoles in the adiabatic potential. Nonadiabatic and exchange-adiabatic effects may also be significant, but are not examined here. The effect of the quadrupole potential on the p -wave and d -wave phase shifts is shown in Table IV, and nowhere exceeds 10%. The quoted dipole-plus-quadrupole phase shifts should be reliable to 1%, within the context of the model, the chief uncertainty again being the value of α_q . Table V gives the $l=3$ and $l=4$ phase shifts in the dipole-plus-quadrupole case. For $l=4$, the effect of the exchange terms on the phase shift was small, and was therefore neglected for $l>4$. Phase shifts for $4 \leq l \leq 10$ in the nonexchange approximation are given in Table VI, and have been computed for all $l \leq 28$ at $k^2 = 0.5, 0.75, 1.0$, and 3.0 Ry.

Phase shifts for electron scattering by Li^+ are given in Table VII. They are in excellent agreement with those obtained by a totally different numerical technique in a one-channel model using a Roothaan Hartree-Fock ground-state wave function for Li^+ , and the same dipole polarization potential,¹⁰ as were the corresponding sets of results^{2,1} for He.

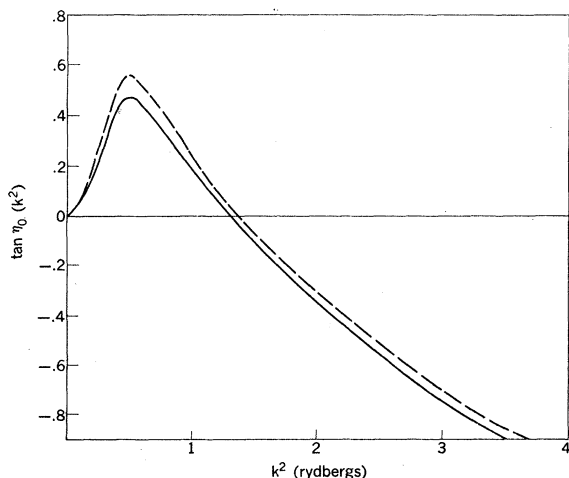


FIG. 3. $\tan \eta_0(k^2)$ for elastic scattering by H^- . Full curve $\alpha_q=0$, dashed curve $\alpha_q \neq 0$.

TABLE VII. Phase shifts for Li^+ , (dipole potential only). (1) Values for $k^2=0$ are obtained by graphical extrapolation. (2) For the p -wave phase shift, the successive columns show the results (i) in our model with $\alpha_d = 0.19$, (ii) in a Hartree-Fock calculation (Ref. 10), (iii) in our model with $\alpha_d=0$.

k^2 (Ry)	$l=0$	$l=1$	$l=1$ HF	$l=1$ $\alpha_d=0$	$l=2$
0	(1.261)	(0.170)	(0.110)	...	(0.0038)
0.04	1.258	0.173	0.113	...	0.0044
0.09	1.255	0.177	0.117	...	0.0052
0.16	1.248	0.182	0.120	0.122	0.0063
0.25	1.241	0.189	0.126	...	0.0074
0.36	1.230	0.195	0.132	0.133	0.0088
0.49	1.221	0.202	0.140	0.140	0.0108
0.64	1.209	0.210	0.147	0.146	0.0135
0.81	1.194	0.217	0.153	...	0.0157
1.0	1.178	0.224	0.161	...	0.0182

This confirms the conjecture made for He that short-range relative $l=0$ correlation in the target is not important.

The extrapolated zero-energy phase shifts $\eta_1(0) = 0.170$ and $\eta_2(0) = 0.0038$ are in good agreement with the corresponding quantum-defect values of 0.148 and 4×10^{-3} . The effect of the dipole polarization potential is, as in the case of He, large.² Calculations¹⁰ to be reported in another paper suggest that the effects of the other multipoles of the adiabatic polarization potential are largely cancelled by the exchange-polarization terms, again as in the case of electron-He scattering.¹ The calculations reported here for H^- and Li^+ may be readily extended to higher members of the isoelectronic sequence for which ground-state wave-function parameters and dipole polarizabilities are available in the literature.^{12,17} Since for electrons on Li^+ the phase shifts obtained in an alternative formulation¹⁰ using a Hartree-Fock Li^+ ground state and the same polarization potential do not differ from those of the present model by more than 1% ($0 \leq k^2 \leq 1.0$ Ry), it was more convenient to carry out the calculations for $Z > 3$ with the Hartree-Fock wave functions, as they are available for more members of the sequence. Such calculations have been performed for the s and p -wave phase shifts (which are needed to evaluate free-free absorption cross sections) for $4 \leq Z \leq 10$. In each case the s -wave phase shift (mod π) is a slowly decreasing function of increasing k^2 ($0 < k^2 \leq 3.0$ Ry), while the p -wave phase is almost independent of energy. Values at threshold and at 1 Ry are given in Table VIII and are sufficiently slowly varying to allow a linear interpolation in that range for $Z \geq 4$. The phase shifts for $Z > 3$ and $l \geq 2$ are very small in this energy range.

Angular Distribution of Electrons Scattered Elastically by H^-

Differential cross sections for elastic scattering of slow electrons by He, in a model closely equivalent to ours, have been reported by Lawson *et al.*³ Those calculated using the phase shifts obtained

TABLE VIII. *s*- and *p*-wave phase shifts for the Li^+ sequence $3 \leq Z \leq 10$ at threshold and $k^2 = 1.0$ Ry. The Li^+ values are computed using Eq. (10a), the others using a Roothaan Hartree-Fock target function; dipole polarization potential only.

$k^2(\text{Ry})$	Z	3	4	5	6	7	8	9	10
10^{-4}	$l=0$	1.261	8.28, -1	6.13, -1	4.87, -1	4.02, -1	3.43, -1	3.00, -1	2.65, -1
	$l=1$	1.70, -1	1.72, -1	1.48, -1	1.27, -1	1.10, -1	9.60, -2	8.56, -2	7.64, -2
1.0	$l=0$	1.178	8.02, -1	6.00, -1	4.81, -1	4.02, -1	3.43, -1	3.00, -1	2.65, -1
	$l=1$	2.24, -1	1.81, -1	1.49, -1	1.27, -1	1.10, -1	9.61, -2	8.56, -2	7.64, -2

in our model are indistinguishable, on the scale of their figures, from the values in Fig. 2 of Ref. 3. No calculations of the angular distributions to be expected in electron scattering by H^- have been published. In view of the oscillatory behavior observed²³ in the scattering of slow protons by nuclei, due to interference between the effects of the repulsive Coulomb force and the nuclear force, it is of interest to examine the behavior in the case of electrons on H^- . Here interference is expected between the repulsive Coulomb scattering and that due to the short-range force (which is dominated by the attractive polarization potential at large r). Since at large r the non-Coulomb part of the potential behaves as $-\alpha_d/r^4$, $\alpha_d \approx 203a_0^3$, many angular momenta should contribute to the non-Coulomb part of the scattering amplitude.

The scattering amplitude may be written as $f(\theta) = f_C(\theta) + f_N(\theta)$ where the Coulomb amplitude $f_C(\theta)$ is given by

$$f_C(\theta) = (1/2k^2) \csc^2 \frac{1}{2}\theta \exp \left\{ i \left[\pi + 2\sigma_0 - 1/k \ln(\sin^2 \frac{1}{2}\theta) \right] \right\} \quad (22)$$

and the non-Coulomb part by

$$f_N(\theta) = \frac{1}{2ik} \sum_{l=0}^{\infty} (2l+1) e^{2i\sigma_l} (e^{2i\eta_l} - 1) P_l(\cos\theta). \quad (23)$$

The differential cross section

$$I(\theta) = |f_C(\theta) + f_N(\theta)|^2 \quad (24)$$

then shows interference effects. It is convenient to examine the ratio $R(\theta, k^2)$ of the calculated differential cross section $I(\theta)$ to that due to the Coulomb repulsion alone, $I_C(\theta) = |f_C(\theta)|^2$. This may be expressed as²³

$$R(\theta, k^2) = |1 + N^2| \quad (25)$$

with (for H^-)

$$N = -2k \sin^2 \frac{\theta}{2} \exp \left\{ \frac{i}{k} \ln(\sin^2 \frac{\theta}{2}) \right\} \times \sum_{l=0}^{\infty} (2l+1) e^{2i\eta_l} \sin \eta_l e^{2i(\sigma_l - \sigma_0)} P_l(\cos\theta). \quad (26)$$

The calculations were carried out at four energies, using the previously calculated phase shifts (both dipole and quadrupole potentials being

included, and the exchange terms being omitted for $l \geq 4$). The real and imaginary parts of N (Eq. 26) were computed separately, the consequent value of $R(\theta, k^2)$ being compared with that obtained from evaluating (22) and (23) directly. The phase-shift program gives σ_l as a byproduct¹⁵: the Legendre functions $P_l(\cos\theta)$ were expressed as polynomials in $\cos\theta$ for $l \leq 4$ and a recursion relation used for higher l . The calculation terminated when the real and imaginary parts of the sum in (26) had converged to a $\frac{1}{2}\%$. For most angles and energies, convergence was comparatively rapid (by $l=14$) but occasionally (for example at $k^2=0.5$ Ry, $\theta=2.60$ radians) as many as 28 terms were required to ensure convergence. If the convergence criterion was relaxed to 5%, convergence was obtained by $l=14$ in all cases.

Calculated values of $R(\theta, k^2)$ at $k^2=0.5$ and 1.0 Ry are shown in Fig. 4. For small k^2 , the ratio $R(\theta, k^2)$ has a slow oscillation in θ after first decreasing to a minimum value, and then rises to a value considerably in excess of unity in the backward direction ($\theta=\pi$). As the energy increases, the first minimum becomes sharper and moves to smaller angles ($\theta=0.45$, $k^2=0.5$ Ry; $\theta=0.40$, $k^2=0.75$ Ry; $\theta=0.36$, $k^2=1.0$ Ry; $\theta=0.22$, $k^2=3.0$ Ry), while the slower oscillations to the large-angle side of the first minimum damp out rapidly with increasing energy. At larger values of k^2 , the first minimum shows some structure, and for $k^2=3.0$ Ry the ratio $R(\theta, k^2)$ first decreases to a value of 3×10^{-2} at $\theta=0.22$, increases to 1.5×10^{-1} at $\theta=0.4$, has a subsidiary minimum of 7.6×10^{-2} at $\theta=0.5$, and then slowly increases to a maximum value of 2.01 at $\theta=\pi$. For comparison, differential cross sections were also calculated at $k^2=0.5$ Ry using the dipole-only phase shifts. They are shown as the dashed curve in Fig. 4(a). The general features are unchanged but the positions of the extrema (in particular the second minimum) shift appreciably, the slow oscillation at intermediate angles having a smaller amplitude, and the backward enhancement is now only a factor of 2.4, rather than 4.0. Although including the quadrupole potential should improve the model, it is clear that the details of the angular distribution at moderate and large angles ($\theta > 0.8$ radians) are sensitive to the model parameters, in particular to the value of the *s*-wave phase shift.

Differential cross sections computed using the dipole-plus-quadrupole phase shifts at $k^2=0.5$ and

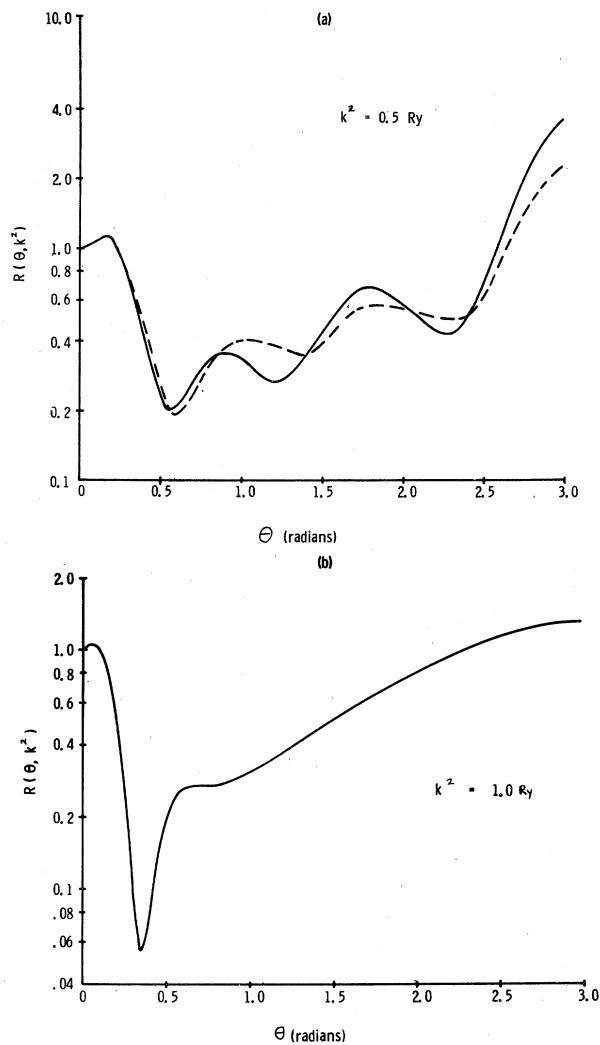


FIG. 4. Calculated values of $R(\theta, k^2)$, the ratio of $I(\theta)$ to the Coulomb intensity $I_C(\theta)$ for H^- , (a) $k^2 = 0.5$ Ry, (b) $k^2 = 1.0$ Ry. The dashed curve in (a) shows the behavior of $R(\theta, k^2)$ when α_q is taken as zero.

1.0 Ry are shown in Fig. 5. It should be noted that the absolute values are large, and the major deviations from the Coulomb differential cross section should be amenable to experimental observation. No account has been taken in this model of inelastic processes. At energies below 0.8 Ry, the only such process energetically accessible is electron detachment $e + H^- \rightarrow e + H(1s) + e$, and although the total cross section for this process may be as large as $40\pi a_0^2$ at $k^2 = 0.5$ Ry, the angular distribution of scattered electrons should be distinguishable from those elastically scattered provided the energy resolution involved is better than 0.75 eV.

Allowing for the uncertainties in the description of the expected angular distribution afforded by the model, the principal features of experimental interest at energies up to 1 Ry, would be the shoulder in the differential cross section in the neighborhood of 30° from the forward direction, and

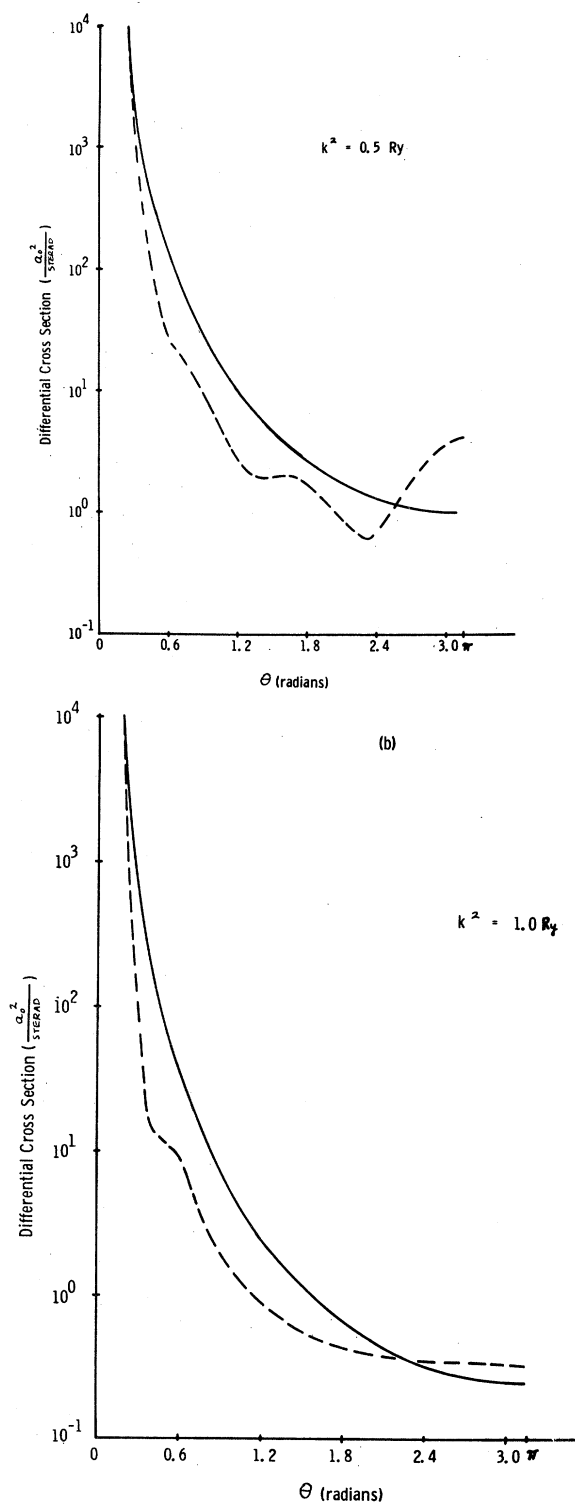


FIG. 5. Calculated differential cross sections for scattering by H^- . The full curve is $I_C(\theta)$, the dashed curve $I(\theta)$. (a) $k^2 = 0.5$ Ry, (b) $k^2 = 1.0$ Ry.

the backward enhancement, which should be more than a factor of two at angles exceeding 160° ($k^2 = 0.5$ Ry). At the lower of the two energies for which differential cross sections are shown in Fig. 5, there is a flat shoulder in $I(\theta)$ near $\theta = \pi/2$,

followed by a deep minimum near $\theta = 3\pi/4$ (when $\alpha_q = 0$, this becomes slightly shallower and shifts to $\theta = 2.4$). The additional structure predicted for $k^2 = 0.5$ Ry is clearly associated with the maximum in the s -wave phase shift (the p -wave phase shift being near $\pi/2$), and as we have seen in Fig. 4(a), is not very model-dependent.

V. CONCLUSIONS

A one-channel model, previously used for elastic scattering of slow electrons by He, has been extended to study elastic scattering by He-like ions. Particular attention is paid to the cases of H^- and Li^+ . In the former case, a long-range repulsive Coulomb interaction is modified by a strong attractive adiabatic polarization potential. This is represented by Bethe-Reeh dipole and quadrupole polarization potentials. Although the Coulomb force is then attractive, the dipole polarization potential remains important in the positive-ion case.

In the case of H^- , the s -wave phase shift which goes to π at zero energy first increases to a maximum value (3.650) at 0.5 Ry and then slowly decreases with increasing impact energy. The omission of the quadrupole potential yields a significantly smaller s -wave shift in the range $0.25 \leq k^2 \leq 2.0$ Ry, but the general behavior is unaffected. The phase shifts for $l \geq 1$ rise smoothly to a maximum value from zero at threshold, and then decrease slowly to zero at high energies. Only the p -wave phase shift reaches $\pi/2$ (near $k^2 = 0.45$ and 2.0 Ry). The effect of including the quadrupole potential on these phase shifts is to slightly increase them (by at most 12%). Exchange effects are negligible for $l > 4$, and the phase shift at fixed energy is a slowly decreasing function of increasing l

($l > 1$).

The Li^+ phase shifts are in reasonable agreement with quantum-defect values at threshold, and are very slowly varying with k^2 in the range $k^2 \leq 3.0$ Ry. As in the case of elastic scattering by He,^{1,2} the phase shifts obtained when a Roothaan Hartree-Fock target wave function is used instead of an open-shell function are unchanged to better than 1%. Hartree-Fock target functions are used therefore to obtain s and p phase shifts for He-like ions up to Ne^{8+} .

The elastic differential cross section for scattering by H^- has been examined at several energies. Results are presented for 0.5 and 1.0 Ry. There are marked departures from Coulomb scattering, particularly at $k^2 = 0.5$ Ry. The general features which include a small value of the ratio $I(\theta)/I_C(\theta)$ near 35° , a clearly shown minimum near 135° , and a strong enhancement in the backward direction do not appear very sensitive to the strength of the quadrupole potential, though the precise angle of occurrence of a given feature and the magnitude of the effect do vary appreciably on going from $\alpha_q = 0$ to $\alpha_q = 1300$.

At low energies ($k^2 < 1.0$ Ry), the differential cross section for $e-H^-$ scattering remains larger than 1.5×10^{-17} cm²/sr at all angles. Measurements of the ratio $R(\theta, k^2) = I(\theta)/I_C(\theta)$ at angles near 35° and 180° , with sufficient energy resolution to reject inelastically scattered and ejected electrons, should be possible and would clearly test the adequacy of the model for the negative-ion case.

ACKNOWLEDGMENTS

Thanks are due to Dr. A. Temkin for helpful suggestions.

*National Academy of Sciences-National Research Council, Senior Post-doctoral Associate.

†On leave of absence from University of Durham, England 1967-8.

¹R. W. LaBahn and J. Callaway, Phys. Rev. **135**, A1539 (1964); **147**, 28 (1966).

²J. H. Williamson and M. R. C. McDowell, Proc. Phys. Soc. (London), **85**, 719 (1964).

³J. Lawson, H. S. W. Massey, J. Wallace, and D. Wilkin, Proc. Roy. Soc. (London) **A294**, 149 (1966).

⁴R. T. Pu and E. S. Chang, Phys. Rev. **151**, 31 (1966).

⁵D. E. Golden and H. W. Bandel, Phys. Rev. **138**, A14 (1965).

⁶L. S. Frost and A. V. Phelps, Phys. Rev. **136**, A1538 (1964).

⁷G. Tisone and L. M. Branscomb, Phys. Rev. Letters **17**, 236 (1966).

⁸D. F. Dance, M. F. A. Harrison, and R. D. Rundel, Proc. Roy. Soc. (London) **A299**, 525 (1967).

⁹J. H. Williamson and M. R. C. McDowell, Phys. Letters **4**, 159 (1963).

¹⁰E. S. Chang, and M. R. C. McDowell, Bull. Am. Phys. Soc. **13**, 615 (1968).

¹¹All quantities will be given in atomic units, the unit of energy being the rydberg, 13.6 eV.

¹²R. D. Hurst, J. D. Gray, G. H. Briguran, and F. A. Matsen, Mol. Phys. **1**, 189 (1958). See also

C. C. J. Roothaan, L. M. Sachs, and A. W. Weiss, Rev. Mod. Phys. **32**, 186 (1960) for the Hartree-Fock wave functions used for $Z \geq 4$.

¹³H. Reeh, A. Naturforsch. **15A**, 377 (1960).

¹⁴M. Abramowitz and I. A. Stegun, Handbook of Mathematical Functions (Dover Publications, N. Y., 1965).

¹⁵A. Burgess, Proc. Phys. Soc. (London) **81**, 442 (1963). For the normalization procedure, see also J. Cooper, Phys. Rev. **128**, 681 (1962).

¹⁶A. L. Stewart, Advan. Phys. **12**, 47 (1963).

¹⁷J. Lahiri and A. Mukherji, J. Phys. Soc. (Japan) **21**, 1128 (1966).

¹⁸P. Swan, Proc. Roy. Soc. (London) **A228**, 10 (1955); private communication.

¹⁹A. Temkin, J. Math. Phys. **2**, 336 (1961).

²⁰M. J. Seaton, Monthly Notices Roy. Astron. Soc. **118**, 508 (1958), N. A. Doughty, M. J. Seaton, and V. B. Sheony, J. Phys. B (Proc. Phys. Soc.) 1968 (to be published).

²¹A. Herzenberg and H. S. N. Lau, Abstracts of the Fifth International Conference on the Physics of Electronic and Atomic Collisions, Leningrad, 1967 (Nauka Leningrad, 1967), p. 261.

²²R. Peterkop, Ref. 21, p. 391.

²³N. F. Mott and H. S. W. Massey, Theory of Atomic Collisions (Oxford University Press, London, 1965), 3rd ed.